

The Kain-Fritsch Convective Parameterization: An Update

John S. Kain*

Cooperative Institute for Mesoscale Meteorological Studies,
University of Oklahoma

To be submitted to
Journal of Applied Meteorology
December 2002

*Also affiliated with the NOAA/National Severe Storms Laboratory

1. Introduction

Convective parameterization continues to be one of the most challenging aspects of numerical modeling of the atmosphere, especially for numerical weather prediction and global climate prediction. A number of convective parameterization schemes (CPSs) have been developed over the years (*e.g.*, Kuo 1974; Arakawa and Schubert 1974; Fritsch and Chappell 1980; Bougeault 1985; Betts 1986; Frank and Cohen 1987; Tiedtke 1989; Gregory and Rowntree 1990; Emanuel 1991; Grell 1993) and many of these schemes continue to be used and modified (*e.g.*, Janjic 1994; Emanuel and Zivkovic-Rothman 1999; Gregory et al. 2000; Grell and Devenyi 2002). One such parameterization is the Kain-Fritsch scheme (Kain and Fritsch 1990, 1993 - hereafter KF), which has been used successfully for many years in the PSU/NCAR mesoscale model (Wang and Seaman 1997; Kuo et al. 1996; Kuo et al. 1997; Cohen 2002) and more recently has been incorporated into experimental versions of NCEP's Eta model (Black 1994), the new Weather Research and Forecasting (WRF) model (Skamarock 2001), and various other models (*e.g.*, Bechtold 2001).

Testing of the scheme within the Eta model has been unique in that it has been carried out in close collaboration with forecasters at the Storm Prediction Center (SPC). A modified configuration of the Eta model, including the KF scheme, has been run at the National Severe Storms Laboratory (NSSL) in a semi-operational mode since 1998. In particular, this configuration (locally known as the EtaKF run) has been run twice daily in parallel with the operational Eta. Output from these forecasts arrive typically about 1-3 h after the operational guidance, well within the window of time during which they have potential to be useful for daily forecasts at the SPC. Scientists from NSSL and CIMMS (Cooperative Institute of Mesoscale Meteorological Studies)/University of Oklahoma have striven to make this output useful to SPC forecasters and feedback from the forecasting unit has played a significant role in assessing model performance (Kain et al. 2003a). This feedback has ultimately led to modifications of the KF scheme and improved forecasts.

The purpose of this Note is to document and describe these modifications as a resource for users of the KF scheme. The modifications are presented within the context of the broader algorithm of the scheme.

2. The “original” Kain-Fritsch scheme

The KF scheme was derived from the Fritsch-Chappell CPS and its fundamental framework and closure assumptions are described by Fritsch and Chappell (1980). Kain and Fritsch (1990) modified the updraft model in the scheme and later introduced numerous other changes, so that it eventually became distinctly different from the Fritsch-Chappell scheme. It was distinguished from its parent algorithm by referring to the more elaborate code as the KF scheme, beginning in the early 1990s (Kain and Fritsch 1993).

These early papers documented many details of the code. Additional details can be found in Bechtold et al. (2001); although this paper describes a significantly modified version of the KF scheme, it documents some sections of the KF code that are not available in print elsewhere, thus it provides a valuable additional reference. Furthermore, a less quantitative description of the code was recently presented in a paper describing one of its unique applications (Kain et al. 2003b). Here, a brief overview of the “old” versions of the code is presented to provide the context for the description of the recent modifications.

The KF scheme is a mass flux parameterization. It uses the Lagrangian parcel method (*e.g.*, Simpson and Wiggert 1969; Kreitzberg and Perkey 1976), including vertical momentum dynamics (Donner 1993), to estimate whether instability exists and, if so, what the properties of convective clouds will be. For the sake of this discussion, it is convenient to compartmentalize the KF scheme into three parts: 1) the convective trigger function, 2) the mass flux formulation, and 3) the closure assumptions. Each of these is discussed briefly below.

a) The trigger function. The first task of the scheme is to identify potential source layers for convective clouds, *i.e.*, updraft source layers (USLs). Beginning at the surface, vertically adjacent layers in the host model are mixed until the depth of the mixture is at least 60 hPa. This combination of adjacent model layers comprises the first potential USL. The mean thermodynamic characteristics of this mixture are computed, along with the temperature and height of this “parcel” at its lifting condensation level (LCL). As a first guess at the likelihood of convective initiation, parcel temperature, T_{LCL} , is compared to the ambient temperature, T_{ENV} at the parcel LCL. Typically, the parcel will be colder than its environment, *i.e.*, negatively buoyant. Based on observations suggesting that convective development tends to be favored by background vertical motion (see Fritsch and Chappell 1980), the parcel is assigned a temperature perturbation linked to the magnitude of grid-resolved vertical motion. The specific formula for this perturbation, δT_{vv} , is

(1)

$$\delta T_{vv} = k(w_g - c(z))^{1/3}$$

where k is a unit number with dimensions $\text{K s}^{1/3} \text{ cm}^{-1/3}$, w_g is the grid-resolved vertical velocity (cm s^{-1}), and $c(z)$ is a threshold vertical velocity given by

$$c(z) = \begin{cases} w_0 \cdot (Z_{LCL}/(2000)), & Z_{LCL} \leq 2000 \\ w_0 & Z_{LCL} > 2000 \end{cases} \quad (2)$$

where $w_0 = 2 \text{ cm s}^{-1}$, Z_{LCL} is the height of the LCL above the ground (m). For example, this equation yields a temperature perturbation of 1 K for a background vertical velocity of 1 cm s^{-1} above the threshold value, and just over 2 K for when w_g is 10 cm s^{-1} above the threshold value.

Use of this perturbation term allows us to effectively eliminate most parcels as candidates for deep convection, which is important for computational efficiency. The elimination process involves adding the computed temperature perturbation (typically 1-2 K, for example, in environments with weak to moderate upward motion) to the parcel temperature at the LCL. If the resulting temperature is still less than the environmental value (*i.e.*, $T_{LCL} + \delta T_{vv} < T_{ENV}$), this parcel is eliminated from consideration. If, however, the perturbed parcel is warmer than its environment, it is allowed to proceed as a candidate for deep convection. At this stage, the parcel is released at its LCL with its original (unperturbed) temperature and moisture content and a vertical velocity

derived from the perturbation temperature. Specifically, its initial vertical velocity, w_{p_0} , is loosely based on the parcel buoyancy equation and is given by

$$w_{p_0} = 1 + 1.1 \cdot [((Z_{LCL} - Z_{USL}) \cdot \delta T_{vv}/T_{ENV})]^{1/2} \quad (3)$$

where Z_{USL} is the height at the base of the USL. This formula yields starting vertical velocities of up to several m s^{-1} .

Above the LCL parcel vertical velocity is estimated at each model level using the Lagrangian parcel method, including the effects of entrainment, detrainment, and water loading (Frank and Cohen 1987; Bechtold et al. 2001). If vertical velocity remains positive over a depth exceeding a specified minimum cloud depth (typically 3-4 km), deep convection is activated using this USL. If not, the base of the potential USL is moved up one model layer and the procedure is repeated. This process continues until either the first suitable source layer is found, or the sequential search has moved up above the lowest 300 hPa of the atmosphere, where the search is terminated. This complete set of criteria comprises the trigger function, but note that the updraft model described in the next subsection plays an important role in determining cloud depth.

b) mass flux formulation. Convective updrafts in the KF scheme are represented using a steady-state entraining/detraining plume model, as described in detail in KF (1990). In this model, entrainment and detrainment rates are inversely proportional, with high entrainment (detrainment) rates being favored by high (low) parcel buoyancy and moist (dry) environments. In practice, the distinction between the updraft and the trigger function can become blurred because the specific formulation of the updraft can determine whether or not the specified minimum cloud depth for deep convection is achieved.

Convective downdrafts are fueled by evaporation of condensate that is generated within the updraft. A fraction of this total condensate is made available for evaporation within the downdraft, based on empirical formulas for precipitation efficiency as a function of vertical wind shear and cloud-base height (Zhang and Fritsch 1986). This fraction effectively dictates the relative magnitudes between downdraft and updraft mass fluxes once other critical downdraft parameters are specified. These other parameters include the downdraft starting and ending levels, its relative humidity profile, and the characteristics and amounts of air that get entrained into the downdraft. The downdraft is specified to start at the level of minimum saturation equivalent potential temperature, θ_{es} , with a mixture of updraft and environmental air. It is moved downward in a Lagrangian sense, with a specified entrainment rate (entraining environmental air only) and a fixed relative humidity of 100% above cloud base and 90% below cloud base. The downdraft is terminated if it becomes warmer than its environment or it reaches the surface. It is forced to detrain into the environment within and immediately above the termination level, such that the minimum depth of the detrainment layer is the same as the minimum depth of the USL, 60 mb.

Environmental mass fluxes are required to compensate for the upward and downward transports in the updrafts and downdrafts, so that the net mass flux at any level in the column is zero. Formulation of these fluxes is described in KF (1993).

c) closure assumptions. The method by which the KF scheme satisfies its closure assumptions is described in Bechtold et al. (2001). Fundamentally, the KF scheme rearranges mass in a column using the updraft, downdraft, and environmental mass fluxes until at least 90% of the CAPE (convective available potential energy) is removed. CAPE is computed in the traditional way, using *undilute* parcel ascent, with the “parcel” characteristics being those of the USL. CAPE is removed by the combined effects of lowering θ_e in the USL and warming the environment aloft.

The scheme feeds back convective tendencies of temperature, water vapor mixing ratio, and cloud water mixing ratio. By default, convective precipitation particles simply accumulate at the surface rather than being introduced aloft, but the code has a “switch” to activate feedback of precipitation at the level it is formed. The switch can be set to any value between 0 (no feedback) to 1 (100% feedback).

3. Recent modifications to the KF scheme

Several different components of the KF scheme have been changed in recent years. They are described individually below.

a. updraft formulation

The algorithm for the KF updraft has been modified with a specified minimum entrainment rate and formulations to allow variability in the cloud radius and cloud depth threshold for deep (precipitating convection). Furthermore, the effects of shallow (non-precipitating) convective clouds are now included as well. These changes and the motivations for making them are discussed below.

1) minimum entrainment rate.

A common criticism from users of the old version of the KF scheme was that it sometimes produced widespread light precipitation in marginally unstable environments and, perhaps as a consequence, it tended to underpredict maximum rainfall amounts within the precipitation area (*e.g.*, Warner and Hsu 2000; Colle et al. 2002). Furthermore, comparison with cloud-resolving model simulations suggested that updrafts were penetrating too far aloft (*e.g.*, Liu et al. 2001). Early testing of the KF scheme in the Eta model corroborated these observations. For example, the scheme often generated widespread “air mass thunderstorms” over the southeastern U. S. during the summer when observed convective activity was isolated or even non-existent.

Diagnostic analysis of the scheme’s behavior revealed that one of the problems was related to the representation of entrainment/detrainment processes. As described in Kain and Fritsch (1990), the rate that environmental air mixes with an updraft is specified in old versions of the scheme, but while some of that air (typically) mixes inward to dilute the mean properties of the updraft, some of it is allowed to immediately detrain back into the environment. If it detrains back into the environment, it does so within turbulent mixtures of updraft and environment, *i.e.*, it carries some updraft air with it. In this way, entrainment and detrainment rates are inversely proportional and they depend on the likelihood that negatively buoyant parcels can be generated when environmental air mixes with the updraft air, including its liquid water or ice. Entrainment of environmental air is favored when updrafts are much warmer than their environment and/or the environment is relatively moist. In this case, negatively buoyant mixtures are less likely because 1) positive buoyancy is large before mixing and 2) evaporative cooling potential is limited by the moist environment. In contrast, when updrafts are marginally buoyant and the environment is relatively dry, detrainment dominates because the evaporative cooling potential is relatively large and relatively little cooling is necessary to induce negative buoyancy.

In the latter type of environment, updraft parcels in the old KF scheme can ascend with very little dilution from the environment. Although the parameterized updrafts shed mass as they ascend, net entrainment is minimized so that mean updraft thermodynamic properties can remain nearly undiluted over a deep layer of ascent. As a result, the unmodified KF scheme has a tendency to allow deep convection to activate too easily when the environmental lapse rate is neutral to slightly unstable, convective inhibition (CIN) is small, and the deep layer RH is low. Further-

more, because the updraft sheds most of its mass and moisture well below the equilibrium level in this circumstance, total condensation and production of precipitation can be quite small.

This problem is largely responsible for the widespread light precipitation sometimes associated with the original KF scheme. It is mitigated in newer versions of the scheme by simply imposing a minimum entrainment rate for the updraft. In particular, the entrainment/detrainment calculations described in KF (1990) are performed initially, but the net environmental entrainment rate, M_{ee} (kg s^{-1} , using the notation of KF 1990), is not allowed to fall below 50% of the total environmental air that mixes into the updraft,

$$M_{ee} \geq 0.5 \cdot \delta M_e, \quad (4)$$

where δM_e is the mixing rate (kg s^{-1}).

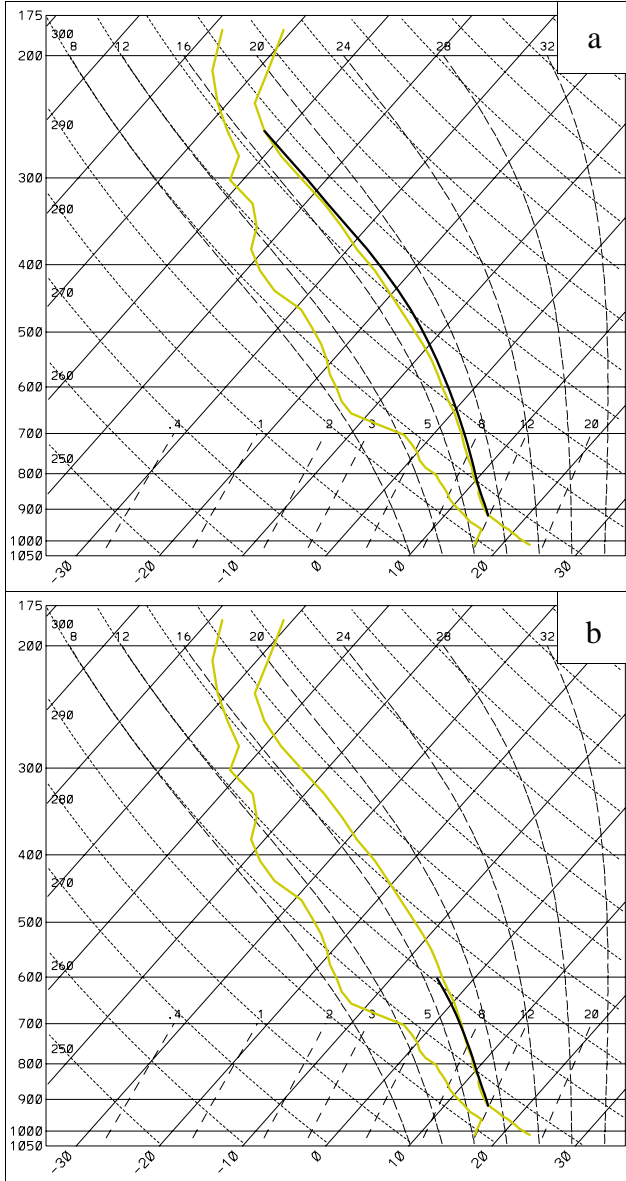


Fig. 1. Predicted updraft path (thick, dark solid line) in a marginally unstable, relatively dry environment using a) the original and b) updated version of the KF scheme.

This change has a significant impact in some environments. For example, Fig. 1a shows the updraft path predicted by older versions of the scheme in one type of marginally unstable, relatively dry environment. The parameterized updraft is only slightly warmer than the environment over a deep layer. In the first 100 hPa or so above cloud base (*i.e.*, \sim the 800 - 900 hPa layer) the environment is relatively moist and the updraft is just starting to accumulate liquid water, so the entrainment process dominates, as reflected by a sharp increase in updraft mass flux (Fig. 2) and a decrease, or dilution, of updraft θ_e (Fig. 3). However, in the relatively dry air of the next \sim 400 hPa, the detrainment processes dominates (Fig. 2) and the updraft undergoes very little dilution (Fig. 3). In contrast, with the mini-

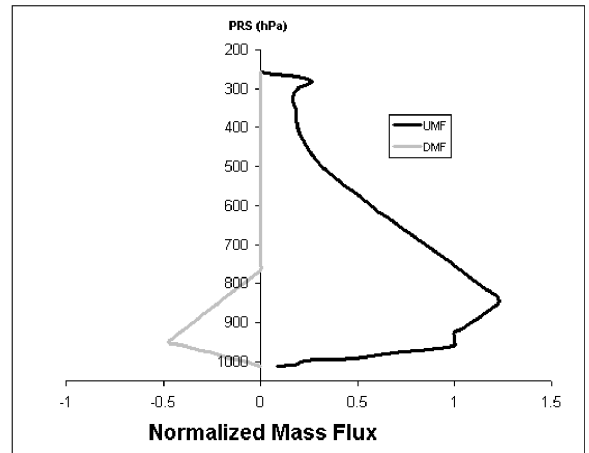


Fig. 2. Updraft mass flux (UMF) predicted by the original version of the KF scheme and downdraft mass flux (DMF) predicted by the updated version of the scheme for the sounding shown in Fig. 1. Both profiles are normalized by the UMF at the top of the USL.

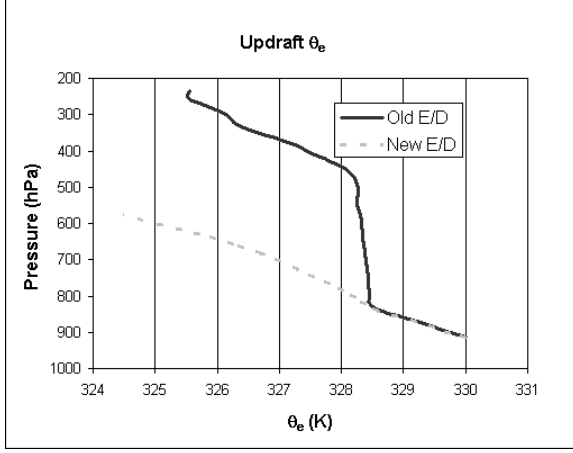


Fig. 3. Updraft θ_e as a function of height (pressure) for the sounding shown in Fig. 1 using the old and new (minimum entrainment) updraft algorithm. Note that the “Old E/D” curve corresponds to updraft mass flux profile shown in Fig. 2.

2) variable cloud radius

In addition to ensuring some dilution of updraft parcels by imposing a minimum entrainment rate, it can be argued that the potential dilution should be a function of larger-scale forcing for convection (Frank and Cohen 1987). In other words, it seems reasonable to introduce additional factors that will promote convective initiation when larger-scale forcing is favorable and suppress initiation when forcing is weak or negative. Indeed, the impact of large-scale destabilizing processes is included (either directly or indirectly) in the closure assumptions of most other CPSs (e.g., Arakawa and Schubert 1974; Anthes 1977; Bougeault 1985; Grell 1993; Janjic 1994; Tiedtke 1989).

As a way of introducing this sensitivity in the KF scheme, a variable cloud radius has been introduced. As indicated in KF (1990) the specified cloud radius, R (m), controls the mixing rate (the maximum possible entrainment rate) according to

$$\delta M_e = M_{u0} \frac{(-0.03 \cdot \delta p)}{R}, \quad (5)$$

where M_{u0} is the updraft mass flux (kg s^{-1}) at cloud base and δp is the pressure depth of a model layer (Pa). In older versions of the KF scheme R is held constant, typically at a value of 1500 m. In the modified code, a conservative attempt to introduce some dependence of R on larger-scale forcing has been included by making it dependent on the magnitude of vertical velocity at the LCL. Specifically, R is defined as

$$R = \begin{bmatrix} 1000, W_{KL} < 0 \\ 2000, W_{KL} > 10 \\ 1000 + \frac{W_{KL}}{10}, 0 \leq W_{KL} \leq 10 \end{bmatrix}, \quad (6)$$

where W_{KL} (cm s^{-1}) is the term inside parentheses in (1), $W_{KL} = w_g - c(z)$. With this modifica-

tion, the *mixing* rate increases as vertical velocity decreases near cloud base. Combined with the minimum entrainment rate (as a fraction of δM_c) discussed above, this typically results in higher dilution of cloud parcels when subcloud layer forcing is weak or negative. It promotes weaker dilution when low-level forcing is stronger.

As implied above, this is a rather conservative (in that R varies over a fairly limited range and never goes below 1000) approach to introducing the fundamental entrainment sensitivity advocated by Frank and Cohen (1987). Furthermore, it is another way of including a sensitivity to deep layer relative humidity in the KF cloud model. It was motivated by evidence that mid-level moisture strongly modulates convective rainfall (*e.g.*, Shepherd et al. 2001) and by observations that the BMJ scheme, in which deep-layer moisture is effectively the trigger function (Baldwin et al. 2002), is quite effective at capturing deep convective activity that is associated with organized mesoscale and larger-scale processes in day-to-day predictions from the Eta model. However, the efficacy of this current formulation appears to be limited because it is dependent on vertical velocity at only one level. Alternative formulations, based on grid-resolved forcing over a deep layer, are being tested.

It should be emphasized that, although cloud radius is the critical parameter in equations (5) and (6), we have little or no skill in actually predicting what the horizontal dimensions of convective clouds in the atmosphere will be. Furthermore, the basic entrainment relationships from which (5) is derived are based on idealized laboratory experiments involving fluids that are quite different from latent-heat driven convective clouds (*e.g.*, see Simpson 1983). The validity of these quantitative relationships for atmospheric convection is tenuous at best (Emanuel 1994 p. 540). Thus, any specific value for cloud radius in (5) should not be taken too literally. Rather, application of (5) should be viewed simply as a mechanism to modulate the rate of dilution, and thereby cloud top, condensation rate, etc., in parameterized clouds. This is consistent with its use in one of the earliest and most enduring convective parameterizations, the Arakawa and Schubert (1974) scheme. In this scheme, R (*i.e.*, the entrainment rate) is systematically manipulated to generate an ensemble of entraining updrafts, such that each model computational level serves as the cloud top for at least one member of the ensemble (Lord 1982).

3) *variable minimum cloud-depth threshold*

Previous versions of the KF scheme used a specified minimum cloud-depth threshold, typically set at 3-4 km. The intention was to delineate between convective clouds that produce precipitation at the surface, and/or a precipitation-induced downdraft, and those that do not. The specified value seemed to work effectively in most situations. However, in semi-operational prediction with the KF scheme in the Eta model (EtaKF), it was noted that this specified value can be inadequate. This was particularly evident in predictions of lake-effect snow, where even casual observations indicated that significant snowfall rates can come from convective clouds that are only around 2 km deep.

In order to allow the KF scheme to parameterize this process, it was deemed necessary to decrease the minimum cloud depth to 2 km. Furthermore, it was reasoned that precipitation production is likely to be favored by active ice phase processes, so that when cloud base temperature is close to 0°C , precipitation is possible with relatively shallow convective clouds. In the absence of a known robust quantitative relationship, it was decided to make the minimum cloud depth a function of T_{LCL} ($^\circ\text{C}$). Specifically, minimum cloud depth, D_{min} (m) is now specified according to

$$D_{min} = \begin{bmatrix} 4000, T_{LCL} > 20^\circ C \\ 2000, T_{LCL} < 0^\circ C \\ 2000 + 100 \cdot T_{LCL}, 0 \leq T_{LCL} \leq 20 \end{bmatrix}. \quad (7)$$

4) Shallow (non-precipitating) convection

Parameterization of shallow convection has long been recognized as an important problem for global climate models (*e.g.*, Browning et al. 1993) and in recent years has become an important concern for mesoscale numerical weather prediction (NWP) models (Gregory and Rowntree 1990; Deng et al. 2003). Parameterized shallow convection transports moisture upward and heat downward within the shallow cloud layer. For NWP and operational forecasting, this process is particularly important because it affects vertical structures, including the boundary layer in some cases, and it often modulates the timing of deep convection initiation. At the SPC, and elsewhere in the National Weather Service, forecasters rely heavily on analysis of model-forecast soundings and these soundings are strongly impacted by parameterized shallow convection in the models (Baldwin et al. 2002). For example, fundamental derived sounding characteristics such as CAPE and CIN (convective inhibition) can be changed dramatically by parameterized shallow convection.

In the modified KF scheme, shallow convection is activated when all of the criteria for deep convection are satisfied *except* that the cloud model yields an updraft more shallow than the minimum cloud depth, similar to the convective schemes in the National Center for Environmental Prediction’s Eta model (Janjic 1994; Baldwin et al. 2002) and the European Centre for Medium-Range Weather Forecasting’s Integrated Forecast System (Gregory et al. 2000). As the trigger function evaluates the potential for deep convection in successively higher USLs within the lowest 300 hPa, the cloud depth associated with each USL that creates any cloud is saved. If deep convection fails to activate, the deepest “shallow” cloud is parameterized. For computational reasons, the value of R is not changed for shallow clouds. The KF (1990) entrainment/detrainment algorithm is used initially to determine cloud properties and mass-flux characteristics, but in the final updraft calculations total mass detrainment is specified to occur as a linear function of decreasing pressure between the LCL and cloud top. So, in effect, the rate of dilution of updraft air is determined by the KF algorithm, but the mass flux and detrainment profiles are specified to be at least qualitatively consistent with large-eddy simulation results (*i.e.*, Siebesma and Cuijpers 1995).

Although shallow convective clouds are, by common definition, non-precipitating, the KF algorithm typically generates precipitation in any cloud deeper than about 50 hPa. If an updraft has already been classified as “shallow”, any precipitation that is generated by the scheme is fed back to resolved scales as an additional moisture source. This is accomplished by setting the “switch” to activate elevated precipitation feedback (see section 2c) to 1.

Parameterized shallow clouds are also modulated by a different closure assumption. In particular, the cloud base mass flux, M_{u0} , is assumed to be a function of turbulent kinetic energy (TKE) in the subcloud layer. This general relationship was initially deduced from physical reasoning rather than quantitative measurements, but recent studies elsewhere have arrived at similar hypotheses regarding the likely relationship between TKE and M_{u0} (*e.g.*, Grant 2001; Neggers et al. 2003). The quantitative relationship in the KF scheme is based on the concept of scaling M_{u0} by the maximum TKE in the subcloud layer. In sampling TKE values from the Eta model’s turbulence parameterization, it was found that boundary layer (assuming most shallow clouds are

driven by surface fluxes) TKE generally varies from $0 \text{ m}^2 \text{ s}^{-2}$ in stable situations to about $10 \text{ m}^2 \text{ s}^{-2}$ in unstable boundary layers with very strong heating from below. Thus, it was decided to assign the maximum value of M_{u0} when $TKE_{MAX} \geq 10$, ramping linearly down to zero when there was no TKE.

But what should the maximum value of M_{u0} be? A normalized updraft mass flux value, UMF^* , has proven to be a useful diagnostic quantity in the KF scheme (Kain et al. 2003b). This quantity is based on the fraction of the USL that is processed by the convective scheme during each convective cycle,

$$UMF^* = (M_{u0} \cdot \tau_c) / m_{USL} , \quad (8)$$

where τ_c is the convective time period, ranging from 1800 to 3600 s and m_{USL} is the amount of mass in the USL (kg). Initial testing associated a value of $UMF^*=1$ with $TKE_{MAX}=10$, *i.e.*,

$$M_{u0} = \begin{cases} \left(\frac{TKE_{MAX}}{k_0} \right) \cdot \left(\frac{m_{USL}}{\tau_c} \right), & TKE_{MAX} < 10 \\ \left(\frac{10}{k_0} \right) \cdot \left(\frac{m_{USL}}{\tau_c} \right), & TKE_{MAX} \geq 10 \end{cases} \quad (9)$$

where $k_0 = 10 \text{ m}^2 \text{ s}^{-2}$, implying that all of the mass in the USL would be processed during a convective cycle when subcloud layer $TKE_{MAX} \geq 10 \text{ m}^2 \text{ s}^{-2}$. Although TKE_{MAX} values typically remain well below $10 \text{ m}^2 \text{ s}^{-2}$ during warm-season diurnal cycles over land, this formulation seemed to produce tendencies that were too strong, so k_0 was increased to 20. This formula seems to produce about the right magnitude of feedback tendencies, judging from the favorable impact in EtaKF forecasts (Kain et al. 2001; Baldwin et al. 2002). For example, Fig. 4a shows the updraft path predicted by the scheme in an environment where deep convection is strongly inhibited.

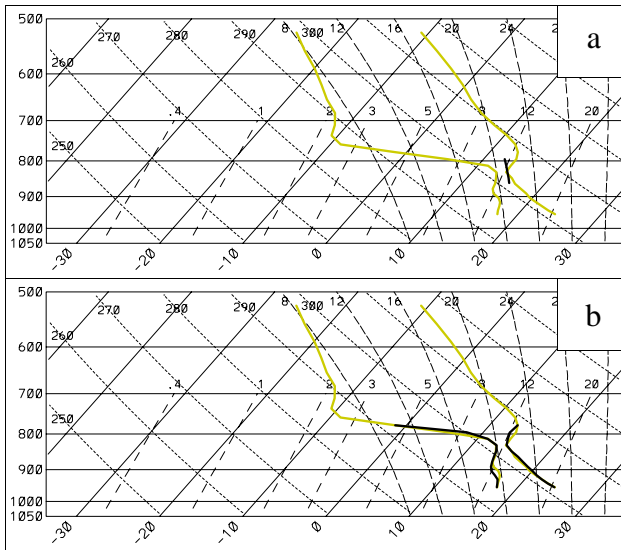


Fig. 4. Parameterized a) updraft path thick, dark solid line and b) convective adjustment profiles (thick dark solid lines) for an environment with strongly capped shallow convection.

In this case, the predicted cloud is less than 1km deep. The maximum subcloud layer TKE is about $5 \text{ m}^2 \text{ s}^{-2}$, so that $M_{u0} \sim 0.25 * M_{USL} / \tau_c$. Maximum temperature and moisture tendencies are on the order of 1 K h^{-1} and $1 \text{ g kg}^{-1} \text{ h}^{-1}$, respectively (Fig. 4b).

Clearly, this formulation could be better calibrated and perhaps adapted to more environmental parameters, such as cloud depth, boundary layer depth, and/or LCL position relative to the top of the boundary layer. Alternatively, an altogether different approach can be taken to implement the same fundamental closure assumption. For example, Grant (2001) argue that cloud-base mass flux for shallow clouds is proportional to the subcloud layer vertical velocity scale, w_* (m s^{-1}), which is closely related to production of TKE and readily available from most turbulence parameterizations.

In particular, they reason that

$$M_{u0} \approx k_1 w_*, \quad (10)$$

where k_1 is a constant with units kg m^{-1} . If this relationship is robust and k_1 can be determined reliably, this would be a very simple closure. At this stage, the relationship between subcloud layer TKE and cloud base mass flux seems to be valid, but more work is needed to better quantify, and perhaps qualify, this relationship and its utility in shallow-convective parameterization (Neggers et al. 2003).

b. Downdraft

Convective downdrafts play an essential role in atmospheric convection. This is quite obvious in the lower troposphere, where downdrafts transport relatively low θ_e air into the subcloud layer and strongly stabilize the local vertical structure. Downdrafts serve this same function in a parameterization scheme. Furthermore, as in the real atmosphere, they can enhance low-level convergence, favoring subsequent convective development at nearby points. However, *parameterized* downdrafts are also important for offsetting updraft mass flux in the lower troposphere. In particular, when downward mass flux is represented in moist, penetrative downdrafts, less environmental “compensating subsidence” is necessary and convective warming and drying tendencies in the lower part of the cloud layer tend to be more realistic (*e.g.*, Johnson 1976; Cheng 1989).

The magnitude of these tendencies, which can have important implications for development of larger-scale precipitation processes and subsequent parameterized convection (Kain and Fritsch 1998), is modulated by the strength (mass flux) of the downdraft relative to the updraft. Consequently, the performance of mass flux CPSs is quite sensitive to parameters that control the ratio of these mass fluxes in the lower troposphere (Tiedtke 1989).

These parameters vary depending on the specific formulation for downdrafts. In general, parameterized downdrafts are driven by condensate from parameterized updrafts. They are typically conceived by an algorithm that determines their depth, (approximately) conserved thermodynamic properties (*i.e.*, θ_e), relative humidity, and the shape of their vertical mass flux profile. Once these properties are known, one can specify either a) the downdraft mass flux value at some level (*e.g.*, Tiedtke 1989; Frank and Cohen 1987) or b) the amount of condensate available for evaporation in the downdrafts (*e.g.*, Fritsch and Chappell 1980; Grell 1993), then solve for the other.

The original KF scheme used the latter approach. It related an overall precipitation efficiency to vertical wind shear and cloud-base height (see Zhang and Fritsch 1986). Its updraft model determined how much condensate was produced and how much of it detrained into the environment, while the empirical precipitation efficiency relationship dictated the fraction of the condensate that reached the surface as precipitation. The remaining condensate was assumed to evaporate in the penetrative downdraft, providing a closure for the specification of downdraft mass flux.

This approach was used for a number of years and the KF scheme has performed quite well with it (*e.g.*, Kuo et al. 1996; Wang and Seaman 1997; Gochis et al. 2002; Cohen 2002), but these precipitation efficiency relationships are difficult to reconcile with observations and cloud modeling studies. The relationship introduced by Fritsch and Chappell (1980), wherein precipitation

efficiency is inversely proportional to vertical wind shear, does not seem to be valid over a wide range of conditions (*e.g.*, Weisman and Klemp 1982; Fankhauser 1988; Ferrier et al. 1996). Furthermore, one can argue that the additional term included by Zhang and Fritsch (1986), relating precipitation efficiency to cloud-base height, is not robust for general applications either. For example, a relatively high cloud base of 3 km can overlay a very dry, unstable convective boundary layer where significant evaporation is likely to occur, but it can also lie at the top of a stable, saturated boundary layer, as is often the case in nocturnal heavy rain events (*e.g.*, Rochette and Moore 1996). The height of cloud base, by itself, is not a reliable indicator of the evaporation rate below cloud base. Finally, even if these relationships were robust, the inverse of precipitation efficiency is not necessarily proportional to the local evaporation rate *in the downdraft*. For example, evaporation in the environment, but outside of lower tropospheric downdrafts, is generally neglected but could be significant (Kreitzberg and Perkey 1976; Emanuel 1991).

Another problem with the KF downdraft formulation is the method of choosing the origination level of downdraft air. The starting level for the downdraft (level of minimum θ_{es} - see section 2b) proves to be quite variable. It is not uncommon for this level to be as high as 300 hPa or as low as 850 hPa. Yet the amount of condensate available for maintaining the specified relative humidity does not change as a function of origination level. For a given amount of condensate and the same detrainment level (usually the surface), a downdraft originating in the mid to upper troposphere is relatively “tall and skinny”, while one starting closer to the surface would be comparatively “short and fat” with the original KF formulation. The corresponding ratios of downdraft to updraft mass flux near cloud base are relatively small (large) in the former (latter) case, implying larger (smaller) parameterized heating and drying rates. Furthermore, the mass of downdraft outflow in the subcloud layer is relatively small for taller updrafts and larger for those originating lower. Thus, the original KF downdraft formulation leads to inconsistent predictions of lower tropospheric heating and drying rates that are not justified by observational evidence or sound physical reasoning. The same is true for the Fritsch and Chappell (1980) approach, although it is somewhat different.

The new downdraft formulation in the KF scheme ameliorates some of these problems. It takes an approach in which key downdraft levels are linked specifically to the updraft. The downdraft is specified to start 150-200 hPa above the USL. This is broadly consistent with most studies on this topic. For example, precipitation-driven downdrafts that penetrate into the subcloud layer appear to originate just above cloud base in relatively weak convective activity (*e.g.*, Betts 1976; Zipser 1977; Knupp and Cotton 1985) and perhaps as much as a few kilometers above cloud base in more intense mid-latitude convection over land (Knupp 1987).

The downdraft is formed entirely from environmental air and it entrains equal amounts of air from all model layers within the downdraft source layer (DSL), which extends from the origination level to the top of the USL. Thus, at the top of the USL it is composed of a mass-weighted mixture of air from each model layer within the DSL. This is distinctly different from the old formulation that extracted most of the downdraft mass from a single origination level. Below the top of the USL, detrainment begins and entrainment ends. The downdraft is allowed to penetrate downward until it reaches the surface or it becomes warmer than its environment. Total detrainment is specified to occur as a linear function of pressure between the top of the USL and the base of the downdraft. Thus, the vertical profile of downdraft mass flux (DMF) shows a sharp peak at the top of the USL and a linear decrease to zero above and below (*e.g.*, Fig. 2).

The downdraft is assumed to be completely saturated above cloud base, with relative humidity decreasing by $20\% \text{ km}^{-1}$ below this level, based loosely on the modeling results of Srivastava

(1985) and widespread observations of subsaturated downdrafts (*e.g.*, Knupp and Cotton 1985). The magnitude of the downdraft mass flux at the top of the USL is specified currently as a simple function of updraft mass flux and relative humidity within the DSL,

$$\frac{DMF_{USL}}{UMF_{USL}} = 2 \times (1 - \overline{RH}), \quad (11)$$

where \overline{RH} is the mean relative humidity in the DSL. This formulation favors “short, fat” downdrafts with maximum mass flux close to cloud base. Environmental humidity is obviously important here, consistent with its important role in determining downdraft strength (Knupp and Cotton 1985) and precipitation efficiency (Ferrier et al. 1996; Shepherd et al. 2001). Since UMF_{USL} depends strongly on lower-tropospheric lapse rates (Kain et al. 2003b), downdraft mass flux is also quite sensitive to environmental stability, another factor emphasized by Knupp and Cotton (1985).

There is no longer a dependence on vertical wind shear. Although wind shear undoubtedly plays a role, especially with regard to precipitation efficiency, this role appears to be quite complex and difficult to isolate from other factors (Fankhauser 1988). In a conceptual sense, wind shear may induce a vertical tilt to updrafts and this may reduce precipitation efficiency (Cheng 1989; Ferrier 1996), but it is questionable whether this effect can be quantified in a useful way for general application. For example, Weisman and Klemp (1982) suggest that precipitation efficiency may be inversely related to wind shear for relatively low instability, low shear environments in which pulse-type (*i.e.*, single cell) convection dominates, but they show that efficiency and shear appear to be positively correlated in environments with higher shear and instability, where mesoscale organization of convection is favored. In the face of this uncertainty about quantitative relationships, it was decided to exclude any dependence on wind shear in the latest version of the KF scheme.

With this downdraft formulation, convective precipitation is given by the residual condensate remaining after updraft detrainment and downdraft evaporation. In some cases, especially those with high cloud bases overlaying a deep convective boundary layer, the algorithm determines that no condensate remains after downdraft evaporation. In this circumstance, no convective precipitation is produced but the scheme is still allowed to activate. Fire-weather forecasters at the SPC are investigating whether predictions of deep convective UMF^* , but no precipitation, correspond to the occurrence of “dry lightning” over the high terrain of the western U. S. (Rich Naden¹, personal communication).

c. Closure Assumption

As discussed in section 2c, the KF scheme uses a CAPE closure. Specifically, it increases mass fluxes incrementally until CAPE is reduced by at least 90%, where CAPE calculations are based on the mean characteristics of air drawn from the USL before and after the parameterized overturning.

In the original KF scheme, CAPE was computed on the basis of undilute parcel ascent, as is typically done for diagnostic calculations. However, it appears that the scheme may overestimate convective rainfall and mass flux (UMF^* - see equation (8)) when it is programmed to eliminate the relatively large positive area corresponding to undilute ascent. For example, the positive area

1. Rich Naden is a Mesoscale Assistant Forecaster at the SPC. His responsibilities include fire-weather forecasting.

for an undilute parcel can be much larger than the area associated with an entraining parcel (cf. Figs. 5 and 1a). In this case, when closure is based on undilute ascent the scheme predicts much larger UMF* and precipitation-rate of the dilute-parcel closure (Table 1). The scheme simply has more CAPE to eliminate when calculations are based on undilute ascent.

In newer versions of the scheme, the closure is based on the CAPE for an entraining parcel. This seems to provide reasonable rainfall rates for a broad range of convective environments and it makes the scheme's UMF* field a better predictor of convective intensity (Kain et al. 2003b).

Table 1:

Closure based on	UMF*	Precip rate (cm h ⁻¹)
undilute ascent	0.60	0.32
Dilute ascent	0.08	0.05

Table 1: Parameterized precipitation rate and normalized Updraft Mass Flux (UMF*) for the sounding shown in Figs. 1 and 5.

4. Summary

A number of modifications have been introduced in the Kain-Fritsch convective parameterization over the last decade or so. The purpose of this paper is to formally describe these changes and provide some justification for their implementation. The changes were inspired by feedback from numerical modelers who use the scheme (*e.g.*, Warner and Hsu 2000; Liu et al. 2001; Colle et al. 2002) and from operational forecasters who utilize model output for daily forecasts (*e.g.*, Kain et al. 2003a). The changes can be briefly summarized as follows:

Updraft

- A minimum entrainment rate is imposed, primarily to suppress convective initiation in marginally buoyant, relatively dry environments. The minimum rate is 50% of the maximum possible entrainment rate defined by Kain and Fritsch (1990)
- The cloud radius, which controls the maximum possible entrainment rate, is specified to vary as a function of subcloud layer convergence, similar to a formulation by Frank and Cohen (1987). This modification suppresses deep convective activation in weakly convergent or divergent environments, and promotes activation in strongly convergent regimes.
- A minimum cloud depth, required for activation of deep convection, is allowed to vary as a function of cloud base temperature rather than remaining constant. This is designed to allow the activation of deep convection for relatively shallow clouds when ice-phase processes are active.
- Shallow (non-precipitating) convective clouds are allowed. They are activated when the scheme's cloud model determines that buoyant updrafts can form but cannot reach the imposed minimum cloud depth for deep convection. Cloud-base mass flux is based on TKE in the sub-cloud layer for shallow clouds, rather than CAPE.

Downdraft

- A new downdraft algorithm is introduced. Downdrafts are formed from air in the layer from 150-200 hPa above cloud base and they detrain over a fairly deep layer below cloud base. Downdraft mass flux is estimated as a function of the relative humidity and stability just above cloud base, but is no longer related to vertical wind shear.

Closure assumption

- The scheme is still programmed to eliminate CAPE, but the calculation of CAPE is based on the path of an entraining (diluted) parcel rather than one that ascends without dilution.

Acknowledgements

This work was partially funded by NOAA-OU Cooperative Agreement #NA17RJ1227 and COMET Cooperative Project numbers O99-15805 and S01-32796. Special thanks goes to Mike Baldwin of CIMMS/OU/NSSL who provided valuable insight in the interpretation of model output and played a critical role in facilitating testing within the Eta model.

REFERENCES

- Anthes, R.A., 1977: A cumulus parameterization scheme utilizing a one-dimensional cloud model. *Mon. Wea. Rev.*, **105**, 270-286.
- Arakawa, A., and W.H. Schubert, 1974: Interaction of a cumulus cloud ensemble with the large-scale environment, Part I. *J. Atmos. Sci.*, **31**, 674-701.
- Baldwin, M. E., J. S. Kain, and M. P. Kay, 2002: Properties of the convection scheme in NCEP's Eta model that affect forecast sounding interpretation. *Wea. Forecasting*, **17**, 1063-1079.
- Bechtold, P., E. Bazile, F. Guichard, P. Mascart, and E. Richard, 2001: A mass-flux convection scheme for regional and global models. *Quart. J. Roy. Meteor. Soc.*, **127**, 869-886.
- Betts, A. K., 1976: The thermodynamic transformation of the tropical subcloud layer by precipitation and downdrafts. *J. Atmos. Sci.*, **33**, 1008-1020.
- Betts, A.K., 1986: A new convective adjustment scheme. Part I: Observational and theoretical basis. *Quart. J. Roy. Meteor. Soc.*, **112**, 677-692.
- Black, T.L., 1994: The new NMC mesoscale Eta model: Description and forecast examples. *Wea. Forecasting* **9**, 265-278.
- Bougeault, P., 1985: A simple parameterization of the large-scale effects of cumulus convection. *Mon. Wea. Rev.*, **113**, 2108-2121.
- Browning, K. A., A. K. Betts, P. R. Jonas, R. Kershaw, M. Manton, P. J. Mason, M. Miller, M. W. Moncrieff, H. Sundqvist, W. K. Tao, M. Tiedtke, P. V. Hobbs, J. Mitchell, E. Raschke, R. E. Stewart, and J. Simpson, 1993: The GEWEX Cloud System Study (GCSS). *Bull. Amer. Meteor. Soc.*, **74**, 387-399.
- Cheng, M.-D., 1989: Effects of downdrafts and mesoscale convective organization on the heat and moisture budgets of tropical cloud clusters. Part II: Effects of convective-scale downdrafts. *J. Atmos. Sci.*, **46**, 1540-1564.
- Cohen, C., 2002: A Comparison of Cumulus Parameterizations in Idealized Sea-Breeze Simulations. *Mon. Wea. Rev.*, **130**, 2554-2571

- Colle, B. A., J. S. Tongue, and J. B. Olson, 2002: Objective verification of the MM5 over the northeast U. S.: Comparison with the NCEP Eta and impact of high resolution. Preprints, 15th Conference on Numerical Weather Prediction, San Antonio, TX, Amer. Meteor. Soc., 89-92.
- Deng, A., N. L. Seaman, and J. S. Kain, 2003: A shallow-convection parameterization for mesoscale models Part I: Sub-model description and preliminary applications. *J. Atmos. Sci.*, in press.
- Donner, L. J., 1993: A Cumulus parameterization including mass fluxes, vertical momentum dynamics, and mesoscale effects. *J. Atmos. Sci.*, **50**, 889-906.
- Emanuel, K. A., 1991: A scheme for representing cumulus convection in large-scale models. *J. Atmos. Sci.*, **48**, 2313-2329.
- Emanuel, K. A., 1994: *Atmospheric Convection*, Oxford University Press, 580 pp.
- Emanuel, K. A., and M. Zivkovic-Rothman, 1999: Development and evaluation of a convective scheme for use in climate models. *J. Atmos. Sci.*, **56**, 1766-1782.
- Fankhauser, J.C., 1988: Estimates of thunderstorm precipitation efficiency from field measurements in CCOPE. *Mon. Wea. Rev.*, **116**, 663-684.
- Ferrier, B. S., J. Simpson, and W.-K. Tao, 1996: Factors responsible for precipitation efficiencies in midlatitude and tropical squall simulations. *Mon. Wea. Rev.*, **124**, 2100-2125.
- Frank, W. M., and C. Cohen, 1987: Simulation of tropical convective systems. Part I: A cumulus parameterization. *J. Atmos. Sci.*, **44**, 3787-3799.
- Fritsch, J.M., and C.F. Chappell, 1980: Numerical prediction of convectively driven mesoscale pressure systems. Part I: Convective parameterization. *J. Atmos. Sci.*, **37**, 1722-1733.
- Gochis, D. J., W. J. Shuttleworth, and Z.-L. Yang, 2002: Sensitivity of the Modeled North American Monsoon Regional Climate to Convective Parameterization. *Mon. Wea. Rev.*, **130**, 1282-1298.
- Grant, A. L. M., 2001: Cloud-base fluxes in the cumulus-capped boundary layer. *Quart. J. Roy. Meteor. Soc.*, **127**, 407-421.
- Grell, G.A., 1993: Prognostic evaluation of assumptions used by cumulus parameterizations. *Mon. Wea. Rev.*, **121**, 764-787.
- Grell, G. A., and D. Devenyi, 2002: A generalized approach to parameterizing convection combining ensemble and data assimilation techniques. *Geoph. Res. Letters*, **29**, 38:1-38:4.
- Gregory, D., and P. R. Rowntree, 1990: A mass flux convection scheme with representation of cloud ensemble characteristics and stability-dependent closure. *Mon. Wea. Rev.*, **118**, 1483-1506.
- Gregory, D., J.-J. Morcrette, C. Jakob, A. C. M. Beljaars, and T. Stockdale, 2000: Revision of convection, radiation, and cloud schemes in the ECMWF Integrated Forecasting System. *Quart. J. Roy. Meteor. Soc.*, **126**, 1685-1710.
- Janjic, Z.I., 1994: The step-mountain eta coordinate model: Further developments of the convection, viscous sublayer, and turbulence closure schemes. *Mon. Wea. Rev.*, **122**, 927-945.
- Johnson, R. H., 1976: The role of convective-scale precipitation downdrafts in cumulus and synoptic-scale interactions. *J. Atmos. Sci.*, **33**, 1890-1910.
- Kain, J. S., and J. M. Fritsch, 1990: A one-dimensional entraining/detraining plume model and its application in convective parameterization. *J. Atmos. Sci.*, **47**, 2784-2802.
- Kain, J.S., and J.M. Fritsch, 1993: Convective parameterization for mesoscale models: The

- Kain- Fritsch scheme. The representation of cumulus convection in numerical models. Meteor. Monogr., No. 24, Amer. Meteor. Soc., 165-170.
- Kain, J.S., and J.M. Fritsch, 1998: Multiscale Convective Overturning in Mesoscale Convective Systems: Reconciling Observations, Simulations, and Theory. *Mon. Wea. Rev.*, **126**, 2254-2273.
- Kain, J. S., M. E. Baldwin, P. R. Janish, and S. J. Weiss, 2001: Utilizing the Eta model with two different convective parameterizations to predict convective initiation and evolution at the SPC. *Preprints, Ninth Conference on Mesoscale Processes*, Ft. Lauderdale, FL, 91-95.
- Kain, J. S., M. E. Baldwin, and S. J. Weiss, P. R. Janish, M. P. Kay, and G. Carbin, 2003a: Subjective verification of numerical models as a component of a broader interaction between research and operations. *Accepted for publication in Wea. Forecasting*.
- Kain, J. S., M. E. Baldwin, and S. J. Weiss, 2002b: Parameterized updraft mass flux as a predictor of convective intensity. *Wea. Forecasting*, in press
- Knupp, K. R., 1987: Downdrafts within High Plains cumulonimbi. Part I: General kinematic structure. *J. Atmos. Sci.*, **44**, 987-1008.
- Knupp, K. R., and W. R. Cotton, 1985: Convective cloud downdraft structure: An interpretive survey. *Rev. Geoph.*, **23**, 183-215.
- Kreitzberg, C. W., D. J. Perkey, 1976: Release of potential instability: Part I. A sequential plume model within a hydrostatic primitive equation model. *J. Atmos. Sci.*, **33**, 456-475.
- Kuo, H.-L., 1974: Further studies of the parameterization of the influence of cumulus convection on the large scale flow. *J. Atmos. Sci.*, **31**, 1232-1240.
- Kuo, Y.-H., R. J. Reed, and Y. Liu, 1996: The ERICA IOP5 storm: Mesoscale cyclogenesis and precipitation parameterization. *Mon. Wea. Rev.*, **124**, 1409-1434.
- Kuo, Y.-H., J. Bresch, M.-D. Cheng, J. S. Kain, D. B. Parsons, W.-K. Tao, and D.-L. Zhang, 1997: Summary of a Mini-Workshop on Cumulus Parameterization for Mesoscale Models. Bulletin of the American Meteorological Society, *Bull. Amer. Meteor. Soc.*, **78**, 475-491.
- Liu, C., M. W. Moncrieff, W. W. Grabowski, 2001: Explicit and parameterized realizations of convective cloud systems in TOGA COARE. *Mon. Wea. Rev.*, **129**, 1689-1703.
- Lord, S. J., 1982: Interaction of a cumulus cloud ensemble with the large-scale environment. Part III: Semi-prognostic test of the Arakawa-Schubert cumulus parameterization. *J. Atmos. Sci.*, **39**, 88-103.
- Neggers, R. A. J., A. P. Siebesma, G. Lenderink, and A. A. M. Holstag, 2003: An evaluation of mass flux closures for diurnal cycles of shallow cumulus. Submitted to *Mon. Wea. Rev.*
- Rochette, S. M., and J. T. Moore, 1996: Initiation of an elevated mesoscale convective system associated with heavy rainfall. *Wea. Forecasting*, **11**, 443-457.
- Shepherd, J. M., B. S. Ferrier, and P. S. Ray, 2001: Rainfall morphology in Florida convergence zones. *Mon. Wea. Rev.*, **129**, 177-197.
- Siebesma, A. P., and J. W. M. Cuijpers, 1995: Evaluation of parametric assumptions for shallow convection. *J. Atmos. Sci.*, **52**, 650-656.
- Simpson, J., 1983: Cumulus clouds: Interactions between laboratory experiments and observations as foundations for models. *Mesoscale Meteorology*. D.K. Lilly and T. Gal-Chen, Eds.,

- Reidel, 399-412.
- Simpson, J. and V. Wiggert, 1969: Models of precipitating cumulus towers. *Mon. Wea. Rev.*, **97**, 471-489.
- Skamarock, W. C., J. B. Klemp, and J. Dudhia, 2001: Prototypes for the WRF (Weather Research and Forecasting) model. *Preprints, Ninth Conference on Mesoscale Processes*, Amer. Met. Soc., Ft. Lauderdale, FL, J11-J15.
- Srivastava, R. C., 1985: A simple model of evaporatively driven downdraft: Application to microburst downdraft. *J. Atmos. Sci.*, **42**, 1004-1023.
- Tiedtke, M., 1989: A comprehensive mass flux scheme for cumulus parameterization in large-scale models. *Mon. Wea. Rev.*, **117**, 1779-1800.
- Wang, W. and N. L. Seaman, 1997: A comparison of convective parameterization schemes in a mesoscale model. *Mon. Wea. Rev.*, **125**, 252-278.
- Warner, T. T., H.-M. Hsu, 2000: Nested-model simulation of moist convection: The impact of coarse-grid parameterized convection on fine-grid resolved convection. *Mon. Wea. Rev.*, **128**, 2211-2231.
- Weisman, M. L., and J. B. Klemp, 1982: The dependence of numerically simulated convective storms on vertical wind shear and buoyancy. *Mon. Wea. Rev.*, **110**, 504-520.
- Zhang, D.-L., and J.M. Fritsch, 1986: Numerical simulation of the meso- β scale structure and evolution of the 1977 Johnstown flood. Part I: Model description and verification. *J. Atmos. Sci.*, **43**, 1913-1943.
- Zipser, E.J., 1977: Mesoscale and convective-scale downdrafts as distinct components of squall-line circulation. *Mon. Wea. Rev.*, **105**, 1568-1589.